

Article

Growth Response of Nine Tree Species to Water Supply in Planting Soils Representative for Urban Street Tree Sites

Alexander Schütt ^{1,*} , Joscha Nico Becker ¹ , Christoph Reisdorff ² and Annette Eschenbach ¹

¹ Institute of Soil Science, CEN Center for Earth System Research and Sustainability, Universität Hamburg, 20146 Hamburg, Germany; joscha.becker@uni-hamburg.de (J.N.B.); annette.eschenbach@uni-hamburg.de (A.E.)

² Institute of Plant Science and Microbiology, Universität Hamburg, 22609 Hamburg, Germany; christoph.reisdorff@uni-hamburg.de

* Correspondence: alexander.schuet@uni-hamburg.de

Abstract: In urban environments, newly planted street trees suffer from poor site conditions and limited water availability. It is challenging to provide site conditions that allow the trees to thrive in the long term, particularly under climate change. Knowledge about the hydrological properties of artificial urban planting soils related to the response of tree species-specific growth is crucial, but still lacking. Therefore, we established a three-year experimental field setup to investigate the response of nine tree species (135 individuals) to two common urban planting soils and a loamy silt reference. We determined and measured soil hydrological parameters and monitored tree growth. Our results revealed low plant available water capacities (6% and 10% v/v) and hydraulic conductivity restrictions with the drying of the sandy-textured urban planting soils. Therefore, tree species that are investing in fine root growth to extract water from dry soils might be more successful than trees that are lowering their water potential. Tree growth was overall evidently lower in the urban planting soils compared with the reference and differed between and within the species. We showed that using unfavorable planting soils causes severe, species-specific growth deficits reflecting limited above-ground carbon uptake as a consequence of low water availability.

Keywords: tree growth; soil water monitoring; relative extractable water; soil water tension; soil water content; urban water management; soil texture; structural soil



Citation: Schütt, A.; Becker, J.N.; Reisdorff, C.; Eschenbach, A. Growth Response of Nine Tree Species to Water Supply in Planting Soils Representative for Urban Street Tree Sites. *Forests* **2022**, *13*, 936. <https://doi.org/10.3390/f13060936>

Academic Editors: Thomas Rötzer, Stephan Pauleit, Mohammad A Rahman and Astrid Reischl

Received: 20 April 2022

Accepted: 13 June 2022

Published: 15 June 2022

Publisher's Note: MDPI stays neutral with regard to jurisdictional claims in published maps and institutional affiliations.



Copyright: © 2022 by the authors. Licensee MDPI, Basel, Switzerland. This article is an open access article distributed under the terms and conditions of the Creative Commons Attribution (CC BY) license (<https://creativecommons.org/licenses/by/4.0/>).

1. Introduction

Establishing newly planted street trees is a critical step to achieve green infrastructure goals and to maintain the tree population in cities. This is particularly challenging, since growing conditions for urban street trees are highly unfavorable [1–3]. Due to anthropogenic transformations and translocations, urban soils exhibit a high degree of spatial heterogeneity. Artificial sandy and stony substrates [4,5], high degrees of soil compaction [1], surface sealing [6,7], and vertical and horizontal limitations of root distribution [8] alter tree sites and, in particular, street tree sites in comparison with natural environments. However, there has been little research on the impact of artificial urban soils on tree growth and the long-term success of new plantings [9]. Climate change and the urban heat island are prolonging the tree growing season and increasing the inner-city atmospheric water deficit, thus raising the transpirational water demand of the trees [10]. As observed in the summers of 2018 and 2019 [11,12], increased meteorological droughts (i.e., phases of deficiency and uneven distribution of precipitation) and storm events with high run-off shares are likely to occur more frequently in Mid-Europe, causing soil water scarcity in cities [13]. Since soil water replenishment by single and few precipitation events at freshly planted tree sites is less effective [14] and successive and frequent precipitation during summer is predicted to decrease in the future climate [15], climate change is likely to exacerbate water limitation and thus the growing conditions of street trees. As a consequence, urban street trees are

likely to grow slower than trees in rural environments and forests [16]. However, direct growth comparisons are sparse, and findings are not consistent [17,18] and seem to be not appropriate to assess the effect level that soil constraints have on the growth of urban street trees. Therefore, on-site comparisons of various tree species and planting soils under identical climate conditions are necessary.

Freshly planted street trees, suffering from transplanting shock, have to adapt rapidly to urban site conditions and reestablish a root:shoot ratio adequate to meet the above-ground demands [19]. This results in low life expectancies of less than 30 years [20] and particularly large premature mortality rates for recently transplanted tree populations from nurseries into urban street sites [21,22]. To achieve fully developed ecosystem services in the long term, these initial growth conditions have to be further improved based on detailed investigations into the interaction of tree growth and urban planting soils with a focus on soil water characteristics. Because street tree sites usually act as multifunctional public spaces, however, the tree's demand itself often takes a secondary role in planning processes. For example, original local or artificial soils are often replaced by technical soil–gravel mixtures (structural planting soils) prior to planting to ensure compaction stability for parking lots and pedestrian infrastructure [23–27]. These structural planting soils contain high percentages of gravel (grain size > 2 mm), amended with soil–compost mixtures (grain size < 2 mm) that are dominated by a sandy texture [5,26]. In addition to often small planting pits [24,28,29] in relation to standards [30], it has to be questioned whether sandy-textured structural soil substrates can ensure sufficient water supply for young street trees [5,14,31], particularly under climate change. However, the hydrology of structural soils and surrounding urban roadside soils and its effect on tree growth potential has not been systematically studied so far [25,29,32].

Tree growth habit is the result of intrinsically determinate reaction patterns to extrinsic factors [16]. Therefore, sandy and coarsely textured planting soils [3,5,33] with comparatively low organic matter contents [34] are expected to significantly affect tree growth rates [1,23,32], but not in a uniform pattern [9]. Depending on the particular hydrological characteristics of their habitat, trees have evolved multiple physiological strategies to counteract substantial vitality loss in situations of limited water availability. Thus, stress reactions can differ quantitatively and/or qualitatively between species. It is still the subject of scientific debates, which strategies of stress reactions are most promising for surviving increasing stress incidences and which main intrinsic factors foster mortality risk [35–38]. Since the drought strategies of particular tree species are yet not fully understood, the suitability of tree species for urban street site planting has been so far mainly determined by meta-studies, assessing the drought resistance of tree species based on the aridity of their natural habitat [39]. A classification according to additional site-specific criteria, such as individual soil requirements for these tree species, is missing [39]. To determine the suitability of tree species and cultivars as urban street trees, long-term observational studies under in situ conditions in different cities have been conducted (e.g., GALK-Straßenbaumtest: <http://strassenbaumliste.galk.de/sblistepdf.php> (accessed on 2 April 2021); [40–42]). However, a conclusive statement regarding the species-specific growth responses to urban planting soils is still missing.

The aim of the present study was to determine the constraints of artificial urban soils on the growth of different tree species with a focus on soil hydrological properties. In particular, we aim to answer the questions: (a) Which hydrological properties and dynamics are characteristic of the selected representatives of urban planting soils? (b) Did periods of critical soil water availability occur in urban planting soils vs. natural soils under the climatic conditions during 2019–2021? (c) Which growth patterns were measurable overall and in the responses of tree species to specific soil conditions? Our approach for a suchlike assessment is to simulate experimentally urban below-ground conditions at one single site to provide identical climatic conditions. Therefore, we established a large-scale experimental field in a complete block design. A total of 135 standardized eight-year-old trees of nine tree species (DBH: 4.5 cm–5.1 cm) were each planted in pits

of 7.5 m³ filled alternately with urban-typical artificial planting soils and one reference (loamy silt). The tree species selection was conducted based on three criteria: (a) general suitability as an urban tree, (b) underrepresentation in Hamburg's (Germany) street tree population, and (c) availability in the tree nursery. The soil hydrological parameters were measured in the laboratory and in the field. Tree growth was monitored morphometrically and dendrometrically for three years.

2. Materials and Methods

2.1. Study Site

The experiment was carried out at an open field site (6000 m²) in a tree nursery located 15 km south of Hamburg, Germany (Baumschule Lorenz von Ehren GmbH & Co. KG; 53°24' N; 9°57' E). The climate shows a marine influence (Koeppen & Geiger: Cfb), with the highest precipitation in summer, a slightly dryer autumn and winter, and low precipitation in the spring season. The long-term annual means (1981–2010) of precipitation and air temperature are 743 mm and 9.6 °C, respectively [43]. The topography is slightly sloping and the groundwater table is below 20 m from the soil's surface. The predominant soil types at the experimental research site are agricultural-affected Cambisols with fine-textured loamy silts above silty sands to pure sands. The water-holding capacity at field capacity (FC; 60 hPa) ranged between 33% and 38% *v/v*, and that at wilting point (WP; 15,000 hPa) ranged between 10% and 15% *v/v* in the upper soil horizons (analysis method in Section 2.4).

2.2. Substrate and Tree Selection

The experimental site was set up in a randomized complete block design of nine tree species planted in three planting soils. Every species–substrate combination was replicated five times (five blocks), resulting in a total number of 135 trees. Two treatment soils represented urban artificial soil conditions along streets: (1) a pure sand ('Sand'), representing artificial urban soils around street tree plantings [5,14], and (2) a one-layer gravel–soil medium (structural planting soil) mixed according to German standardized guidelines [30], similar to 'Amsterdam Tree Soil' [44] and commonly used as backfill material at newly planted tree sites ('FLL'). The reference soil was supposed to represent optimal growing conditions. Therefore, we used a regional harvested natural topsoil similar to the Cambisols at the experimental site, which were considered very suitable for the production of trees in the nursery and for years have provided good yields and quality ('Loamy Silt'). Planting pits with dimensions of 2.5 m × 2.5 m × 1.2 m (7.5 m³) were excavated for each tree studied. The planting pits were arranged in a 4 × 35 grid with spacing from center to center of 3.5 m × 8 m (Figures S1 and S2).

The tree species were selected on the basis (1) of long-term observational and literature-based studies focusing on the suitability of diverse native and non-native tree species as urban trees (GALK (Table 1) and KLAM [39,45] (Table 1)). Nine tree species were selected from a wide range of tree species and cultivars rated in GALK (*n* = 178) and KLAM (*n* = 235). To achieve greater variability in the growth response patterns, we selected not only the highest-scoring tree species, but also the overall tree species that differed in their scores for drought tolerance (Table 1). Additional criteria for tree selection were (2) an underrepresentation within Hamburg's street tree population as the trees were mostly not yet commonly planted and (3) the availability of the same-sized and aged trees cultivated at the same nursery to provide comparability for the former growing conditions. This resulted in the selection of the following nine tree species: *Tilia cordata* 'Greenspire' (Tc), *Quercus cerris* (Qc), *Quercus palustris* (Qp), *Carpinus betulus* 'Lucas' (Cb), *Ostrya carpinifolia* (Oc), *Gleditsia triacanthos* 'Skyline' (Gt), *Liquidambar styraciflua* (Ls), *Amelanchier lamarkii* (Al), and *Koelreuteria paniculata* (Kp) (Table 1).

Table 1. Tree species characteristics. Planting diameter at breast height (DBH in May 2019) and suitability classifications of the investigated tree species for use as street trees. STP HH is the actual percentage of the investigated tree species from Hamburg’s total street tree population (state: 31 December 2020). Stock of tree species is listed according to age class: The tree species were determined via the Hamburg tree cadaster and show the street tree population according to age classes classified by planting year after 2010, between 1990 and 2010, and before 1990.

Tree Species ‘Cultivar’	Code	DBH (cm)	Suitability		STP HH ³ (%)	Stock of Tree Species ³		
			KLAM ¹	GALK ²		>2010	1990–2009	<1990
<i>Tilia cordata</i> ‘Greenspire’	<i>Tc</i>	5.1 ± 0.1	2.1	Well suited	1.3	737	1561	596
<i>Quercus cerris</i>	<i>Qc</i>	4.6 ± 0.2	1.2	Well suited	0.4	588	113	263
<i>Quercus palustris</i>	<i>Qp</i>	5.3 ± 0.1	2.2	Partly suited	0.9	400	720	924
<i>Carpinus betulus</i> ‘Lucas’	<i>Cb</i>	4.6 ± 0.1	2.1	In test	<0.1	61	0	0
<i>Ostrya carpinifolia</i>	<i>Oc</i>	4.5 ± 0.2	1.1	Suited	0.1	187	90	0
<i>Gleditsia triacanthos</i> ‘Skyline’	<i>Gt</i>	5.1 ± 0.1	1.2	Well suited	0.1	153	98	1
<i>Liquidambar styraciflua</i>	<i>Ls</i>	4.9 ± 0.4	2.2	Suited	0.3	352	155	54
<i>Amelanchier lamarckii</i>	<i>Al</i>	5.0 ± 0.1	3.1	n.d.	0.1	52	53	78
<i>Koelreuteria paniculata</i>	<i>Kp</i>	5.1 ± 0.2	1.2	Partly suited	<0.1	28	2	0

¹ KLAM = Climate Tree Species Matrix. Source: [39,45]. ² GALK = Deutsche Gartenamtsleiterkonferenz (GALK e.V.; German Garden Agency Directors Conference). Source: <http://strassenbaumliste.galk.de/sblistepdf.php> (accessed on 2 April 2021). ³ Source: Free and Hanseatic City of Hamburg, Department for the Environment, Climate, Energy and Agriculture.

In order to create representative conditions for urban tree sites to be planted, the dimensions of the selected trees at the planting date were in accordance with standards. The trees had, therefore, similar initial stem diameters between 4.5 and 5.3 cm at breast height (Table 1). The selected study trees were harvested with a tree digger according to the B&B method (root ball excavated and burlap-wrapped [46]). Therefore, the volume of each root ball was almost similar, with maximum root ball dimensions of 0.5 m × 0.6 m × 0.5 m (0.1 m³). Single trees were planted in the excavated planting pits after the backfilling of the pits with the planting soils (Figures S1 and S2). The planting soils were moderately compacted by consistently trampling throughout the backfilling process. After the first winter, small depressions caused by natural settling at the corners of the planting pits were refilled with the respective soil material. To ensure tree establishment in the early post-transplantation phase, we applied four irrigations using ‘tree gator’ watering bags (approx. 60 L) during the first year. Fertilization (NPK, Mg, and micronutrients (Mn and Zn)) was applied in spring 2020 and 2021 to minimize differences in the initial nutrient concentrations (‘Sand’ lowest and ‘Loamy Silt’ highest) and thus to minimize nutrient-related effects on tree growth.

2.3. Soil Water Monitoring and Meteorological Data

We installed a monitoring setup consisting of soil water potential sensors (SWP; WATERMARK 200SS, Irrometer Inc., Riverside, CA, USA), volumetric water content probes (VWC; CS-650, Campbell Scientific Ltd., Bremen, Germany; Theta Probe ML2x; Delta-T Devices Ltd., Cambridge, UK), and soil temperature sensors (Irrometer Inc., Riverside, CA, USA). The data were logged at hourly intervals by WATERMARK M900 Monitors for SWP and soil temperature sensors (Irrometer Inc., Riverside, CA, USA), with CR-1000 data loggers for the CS-650 VWC sensors (Campbell Scientific Ltd., Bremen, Germany) at plots with *Qc* and with DL18 data loggers for the ML2x VWC sensors (Ecomatik, Dachau, Germany) at plots with *Al* and *Oc*. The monitoring setup on the experimental site was structured as follows: intensive monitoring at one plot of three tree species per planting soil (9 plots; tree species: *Qc*, *Al*, and *Oc*) and extensive monitoring at one plot of all tree species per planting soil (27 plots). The intensive monitoring covered eight SWP sensors with two replicates per depth (10 cm, 35 cm, root-ball, and 100 cm) and four VWC probes without replication at the same depths. The extensive monitoring covered four SWP sensors

without replication, also at the same depths. Temperature sensors were installed next to the SWP and VWC sensors within four randomly chosen plots per planting soil. Soil temperature sensors were installed to allow correction for temperature's effect on SWP measurements. We installed the sensors simultaneous to the backfilling of the planting soils at the predefined depths. For installing the root ball sensors, the root balls were placed at approximately 40 cm depth and covered with the planting soils up to half, where the sensors were placed. Except for the root ball sensors, all sensors were placed with a distance of 75 cm from the horizontal center of the planting pit. The 36 monitoring plots were randomly distributed over the experimental site.

Meteorological data were recorded within one replication block in the middle of the experimental site by a meteorological station (Campbell Scientific, Logan, UT, USA). The air temperature and relative humidity were measured at 2 m height (HMP155A, Vaisala, Vantaa, Finland). For precipitation measurements, we used a tipping bucket rain gauge (52203, R.M. Young Co., Traverse City, MI, USA). All data were recorded within a 15 min interval using a CR-1000 data logger. The atmospheric vapor pressure deficit (VPD) was calculated as the difference between the saturated and actual vapor pressure using the daily means of air temperature and relative humidity.

2.4. Soil Physical Characteristics

We took disturbed and undisturbed soil samples from one plot of each planting soil in November 2019 after the first growing season. The undisturbed soil samples were analyzed in the lab for the fine soil texture composition, coarse soil content (gravel content), total and organic C contents, and soil pH (CaCl_2) (Table 1). The water retention characteristics were assessed using undisturbed soil samples (soil cores of 100 cm³ and 250 cm³) for lab measurements. To derive the water retention curves, the water contents at characteristic pressure levels of pF 0.5, 1.3, 1.8, 2.1, 2.48, 3.48, and 4.2 were measured as a percentage of weight using pressure plate apparatus. Additionally, the water retention characteristics and unsaturated conductivity were determined with 250 cm³ undisturbed soil samples using the fully automated measuring and evaluation system HYPROP [47,48]. The bulk density was determined by drying and weighing these undisturbed volumetric soil samples. Based on the calculated daily means of the measured SWP and VWC data, we also plotted the field retention curves for the three planting soils. The van Genuchten parameters for the functions of the three approaches were determined according to [49] to describe the relationship between VWC and SWP. The data pairs of water contents at levels of pF 0.5, 1.3, 3.48, and 4.2 of the pressure plate method were added to supplement the curves of the HYPROP measurements and the field retention curves, as the measuring devices for these methods had limited measurement ranges. In spring 2020, the infiltration capacities of the planting soils were measured using a double-ring infiltrometer. In order to quantitatively evaluate and compare the soil hydrological characteristics of the three planting soils, we considered the variables of the plant-available water capacity (PAWC), field capacity (FC), infiltration capacity (IC), and unsaturated hydraulic conductivity (K_s).

2.5. Vitality Assessment and Tree Growth Measurements

We assessed the tree vitality by visual inspections of each individual tree regularly at the beginning of September 2020 and 2021. Criteria leading to the vitality score (1, very vital–5, strongly impaired) were (1) the overall leaf conditions and (2) the crown density in comparison with a vital tree of the same species. The assessment followed a regular inspection scheme developed by the GALK (Deutsche Gartenamstleiterkonferenz e.V.).

The stem growth and current-year shoot length were used as indicators for tree performance in the three planting soils. We measured the stem circumference of all trees at heights of 100, 130, and 150 cm in May 2019, January 2020, January 2021, and October 2021 to a decimal place using a measuring tape. Shoot growth was measured in September 2020 and September 2021. Five main external, sun-exposed branches per tree were randomly chosen and the shoot increment was measured in length. The annual average stem increment and

shoot extension for each tree species per substrate were calculated as the average of all sampled replicates.

To study the tree species' reaction to short-term changes in the environmental conditions by measuring continuously the intra-annual stem diameter variation, we installed 23 electronic point dendrometers (DD-L2, Ecomatik, Dachau, Germany; accuracy of $\pm 1.97 \mu\text{m}$ and temperature coefficient $< 0.2 \mu\text{m K}^{-1}$) in spring 2021. For dendrometer installation, three individual trees per species (with the exception of *Qc* (only $n = 2$) and *Kp* (no measurements)) growing in the planting soil 'Sand' were selected. At each tree, the dendrometers were installed with the dendrometer head on the outer bark at approximately 110 cm stem height. The sensors measured with a frequency of 15 min and were connected to both CR-1000 and DL-18 dataloggers.

2.6. Data Processing

The monitored SWP data were manually corrected for the actual soil temperatures using the in situ soil temperature measurements from the three planting soils [50,51]. The corrected data extended the lower measurement range of -2500 hPa , as $10 \text{ }^\circ\text{C}$ instead of a default value of $24 \text{ }^\circ\text{C}$ was initially set as the constant temperature for logger internal temperature correction. To detect water stress conditions and to quantify the annual duration of critical soil water availability, we used the monitored SWP data below -63 hPa and transformed them into the volumetric water content data using the van Genuchten water retention functions [49] determined for each planting soil (VWC_{vG}). Thereafter, the relative extractable soil water content (REW%) was calculated from the VWC_{vG} depth weighted for a soil compartment from 0–35 cm and depth weighted for a soil compartment from 0–100 cm according to [52]:

$$\text{REW (\%)} = 100 \cdot ((\text{VWC}_{\text{actual}} - \text{VWC}_{\text{WP}}) \cdot (\text{VWC}_{\text{FC}} - \text{VWC}_{\text{WP}})^{-1}) \quad (1)$$

where VWC_{PWP} is the VWC_{vG} at the wilting point and VWC_{FC} is the VWC_{vG} at field capacity, both measured in the lab using the pressure plate method. In the literature, water stress conditions are assumed to occur when the REW drops below the threshold of 40%, as transpiration is gradually reduced due to increasing stomatal diffusion resistance [53]. Therefore, based on the calculated daily means, we calculated the number of days per growing season when $\text{REW} < 40\%$ to seasonally characterize water stress according to [52].

The stem circumference measurements were height-related-transformed to the stem diameter increment at breast height (DBH), assuming a circular stem area. Data processing of the intra-annual stem diameter variations (SDV) was performed using R v. 4.2.1 [54] with the package *treenetproc* [55]. The workflow of *treenetproc* converts raw data (L0) into time-aligned time-series data (L1 data, in this study with hourly resolution), cleans the L1 data from outliers and data shifts, and linearly interpolates data gaps $< 30 \text{ min}$ (L2 data). From the L2 data, we extracted three relevant seasonal proxies [55]. (1) The reversible, water-induced shrinkage and expansion of the stem diameter (maximum daily shrinkage (mds in $\mu\text{m d}^{-1}$)). (2) The irreversible diametric expansion due to woody cell formation with the zero-growth concept, transformed into relative values for better comparison (stem diameter increment (SDI in % of seasonal maximum stem diameter)) [56]. Thus, contrary to [57], no negative growth—due to a smaller diameter maximum on the following day—was considered in the analysis. (3) The tree water deficit (TWD), derived on a daily basis from the maximum precedent stem diameter and actual (daily) maximum stem diameter, represented the missing water in $\mu\text{m d}^{-1}$ [56]. Analyzing the response of intra-annual tree growth on soil hydrological and climate variables is only reliable within the main period of stem growth [58]. Since *treenetproc* returns values for onset and cessation starting from the second year only [55], we determined the length of the growing season of the instrumented trees ($n = 23$) as follows: onset of growth was reached when the actual daily growth rate at least equaled the seasonal average daily growth rate for at least seven consecutive days (period of 1 May 2021 to 30 September 2021). Growth cessation was, therefore, reached when the seasonal average daily growth rate was exceeded for the last time by the actual

daily growth rate on at least seven consecutive days. As we expect mds in contrast to SDI to be a parameter reflecting the trees' water status in the short term, we used daily values for mds to analyze relationships with environmental parameters and weekly means for SDI [57].

2.7. Statistical Analysis

The annual duration of temporal water stress conditions (number of days with REW < 40%) was compared between the three planting soils and the years 2020 and 2021 using a two-way ANOVA. The stem diameter increment and shoot growth as mean values for the years 2020 and 2021 were compared separately (a) within a species between the three planting soils and (b) between all species within each planting soil using a one-way ANOVA. All group means were compared using Tukey's post hoc comparison at p -level ≤ 0.05 .

For analyzing the relationships of the weekly SDI and mds with the environmental variables REW% in 0–35 cm and 0–100 cm depth, precipitation, and VPD, single-factor correlations were calculated and the Spearman's correlation coefficient were reported. The environmental variables for the correlation analysis with SDI were also calculated as calendar week means.

Statistical analyses were conducted using OriginPro v2021b (OriginLab Corporation, Northampton, MA, USA) and R v4.1.2 [54].

3. Results

3.1. Substrate Characteristics

The fine texture (<2 mm) of the urban planting soils 'Sand' and 'FLL' composed predominantly of sandy grains (0.063–2 mm), whereas the dominant fine texture grain size of the 'Loamy Silt' was silt (2–63 μ m) (Table 2). The structural planting soil ('FLL') was composed of 20% v/v gravel. The organic matter content of all investigated soils was below 1% w/w , whereas the 'Sand' had almost no organic matter (<0.1% w/w) and the organic matter content in the 'FLL' was 0.6% w/w . All soils were backfilled into the planting pits loosely compacted to bulk densities between 1.4 and 1.44 $g\ cm^{-1}$. The plant available water capacity (PAWC) of the 'Loamy Silt' was highest, with 23% v/v , corresponding to 1725 L per planting pit (Figure 1a). Compared to the 'Loamy Silt', the plant available water capacity of 'FLL' was <50% and <25% for 'Sand' (773 L per planting pit and 450 L per planting pit, respectively). The total pore volumes of the planting soils 'Sand' and 'Loamy Silt' were the same, at approximately 40% v/v , whereas the total pore volume of the planting soil 'FLL' was 32% v/v . The slope of the 'Loamy Silt' soil-water-retention curve was almost linear in the FC range, while in both artificial soils, the retention curve approached an exponential slope. The soil hydraulic conductivity of 'Sand' declined sharply at REW 75% (Figure 1b). The hydraulic conductivity in 'FLL' was constantly lower and fell below the hydraulic conductivity of 'Loamy Silt' at WP (100% REW) already before 70% REW. Although the hydraulic conductivity in 'Loamy Silt' compared with 'Sand' and 'FLL' had constantly lower values in the wet soil (>10% VWC) (Figure 1a), unsaturated conductivity of $>10^{-5}\ cm\ d^{-1}$ was provided within the whole range of PAWC until WP.

Table 2. Soil properties of the three planting soils with OM as the organic matter content, BD as the bulk density, IC as the infiltration capacity, FC as the field capacity, and PAWC as the plant available water capacity.

Planting Soil	Fine Tex. < 2 mm			Coarse Tex. > 2 mm		OM (v/v)	pH CaCl ₂	BD ($g\ cm^{-1}$)	Hydrological Properties		
	Sand (v/v)	Silt (v/v)	Clay (v/v)	(w/v)	(v/v)				IC ($cm\ min^{-1}$)	FC (v/v)	PAWC (v/v)
'Sand'	95	4	1	2	n.d.	0.1	6.8	1.4	1.5	9.1	6.0
'FLL'	93	5	2	35	20	0.6	6.5	1.4	1.9	14.6	10.3
'Loamy Silt'	29	61	10	1	n.d.	0.9	5.7	1.4	0.3	33.0	23.0

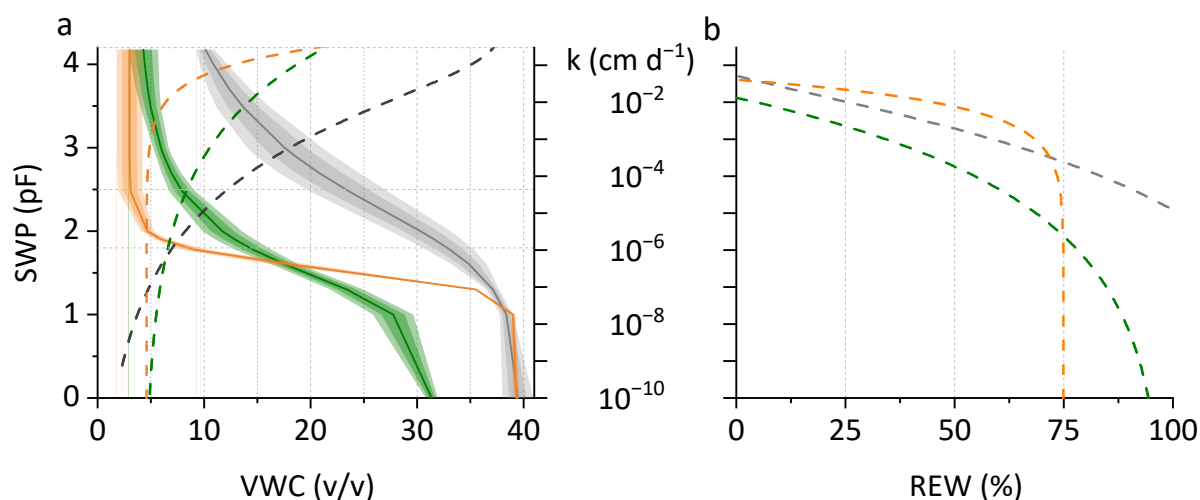


Figure 1. (a) Mean planting soil water retention curves (left y-axis) determined by pressure chamber, HYPROP, and field measurements in the three planting soils ‘Sand’ (orange), ‘FLL’ (green), and ‘Loamy Silt’ (grey). SWP is the soil water potential and VWC is the volumetric water content. Shaded areas highlight the standard deviation (light) and the standard error (dark). Dashed lines show the log-transformed fitted hydraulic conductivity (k) (right y-axis) as a function of VWC determined by the HYPROP apparatus; (b) log-transformed fitted hydraulic conductivity (k) as a function of the REW (relative extractable water) determined by the HYPROP apparatus.

3.2. Environmental Conditions and Soil Water Availability

Compared to the mean 30-year growing season precipitation (May–September 1981–2010; DWD Station Hamburg-Neuwiedenthal) of 343 mm, the years of 2019 to 2021 were slightly dry years (231 mm, 231 mm, and 299 mm, respectively). With the beginning of the growing season in 2019, the root balls in all planting soils strongly dried below the REW 40% threshold value (Figure 2). Irrigation replenished the root balls for short phases. Until the end of the growing season of 2019, the REW in the planting pits remained high in all three planting soils above the threshold value of 40%. During the growing season of 2020, three distinct dry out phases (each > 16 days) occurred, interrupted by replenishing precipitation events.

The first phase was characterized by strong soil water depletion below the water stress threshold only in the root balls. Subsequently, two dry periods led the average REW to drop below the threshold even within the planting soils, prioritized at 10 and 35 cm depths, indicating that tree roots then tapped water from the planting soils in the top soil layer. In 2021, two dry phases occurred, with the REW within the root balls being almost completely depleted and the soil water storage within all planting pits being minimized. However, in ‘FLL’ and ‘Sand’, the soil water storage was replenished by drought-breaking precipitation events, while soil drying in ‘Loamy Silt’ continued. Despite the higher precipitation in 2021, the soil water storage at 0–100 cm depth was depleted below the threshold of 40% REW on evidently more days ($p \leq 0.001$) compared with 2020, indicating progressing root density. Differences in drought incidence between the planting soils were not significant, but we observed a clear tendency of a reduced amount of water stress days in ‘Sand’ during 2021 (Figure 3).

3.3. Tree Growth Analysis

Across all investigated species, annual growth was highest in ‘Loamy Silt’ and lowest in ‘Sand’ (Figure S3). Overall, the annual stem diameter increment was highest during 2021, whereas the annual shoot growth was greatest during 2020 (Figure S3). The lowest values and no significant differences between species and planting soils were measured in 2019. The growth responses of the investigated tree species in the three planting soils varied strongly (Figure 4a). In ‘Loamy Silt’, Q_c and T_c showed the highest growth, whereas

Ls and *Kp* showed the lowest growth. For the DBH growth response toward the planting soils, we identified four general patterns:

1. Significant difference in DBH growth between all three planting soils (*Tc* and *Qp*);
2. Significantly less DBH growth only in 'Sand' (No significant difference between 'FLL' and 'Loamy Silt' (*Oc*, *Ls*, and *Al*);
3. Significantly less DBH growth in 'Sand' and 'FLL' than in 'Loamy Silt' (*Qc*, *Cb*, and *Gt*);
4. No difference in DBH growth between all planting soils (*Kp*).

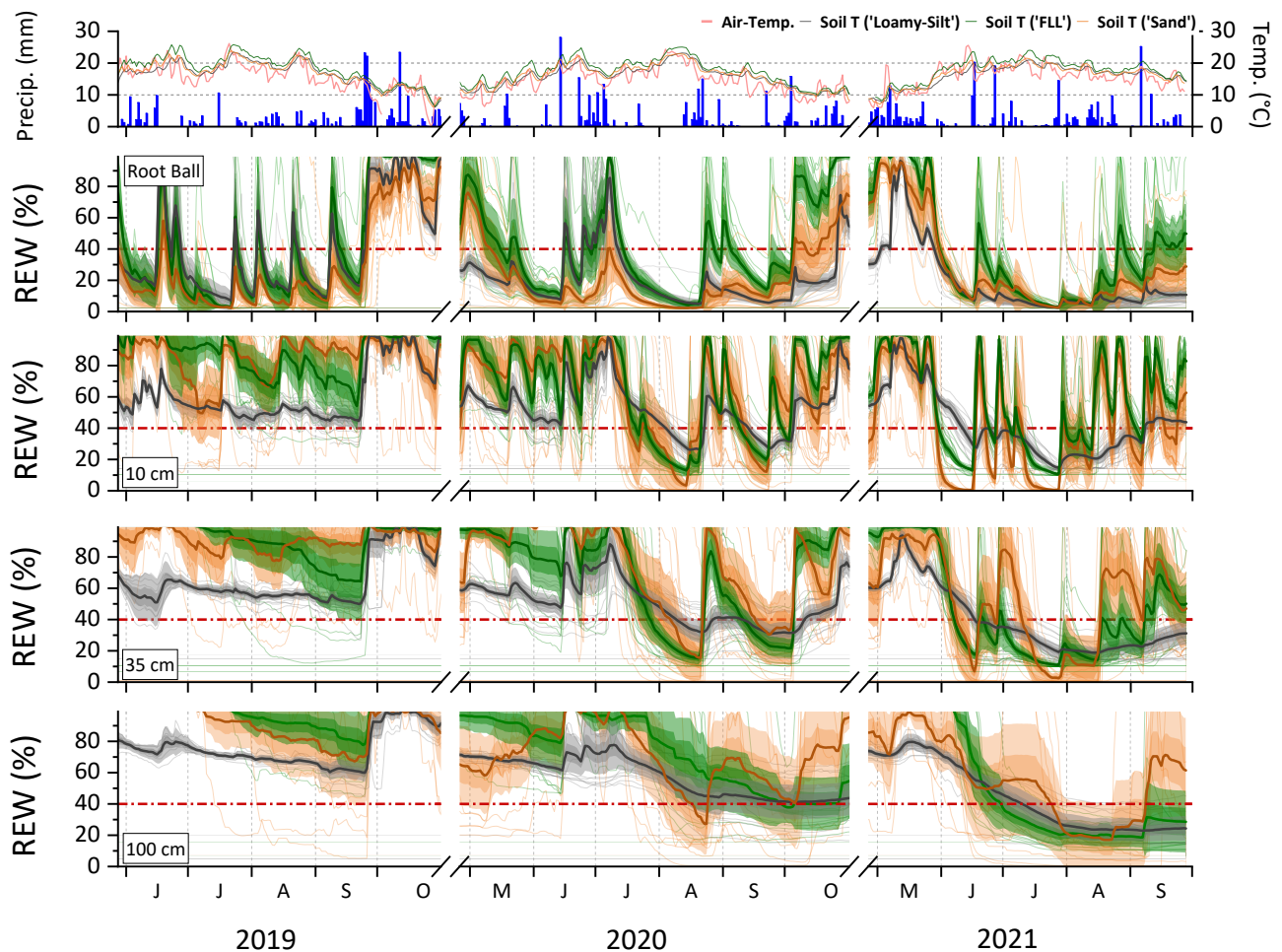


Figure 2. Dynamics of relative extractable water (REW %) at three depths and within the root ball in the three different planting soils ('Sand' (orange), 'FLL' (green), and 'Loamy Silt' (grey)) during the growing seasons of 2019, 2020, and 2021. Bold lines represent the means of all investigated planting pits per planting soil. Shaded areas indicate the standard error (dark) and the standard deviation (light). Reddish dashed lines show a threshold value of 40% REW. Corresponding precipitation, air, and soil temperatures are given at the top of the graph.

Across all species, the tree DBH growth on 'Sand' and 'FLL' was, on average, -64% and -29% , respectively, lower compared with that on the optimum planting soil. *Kp* was excluded from the comparison. On 'Sand', *Qp* and *Al* were most restricted (-85% and -81% , respectively), whereas *Tc* and *Gt* were the less negatively affected species (-44% and -54% , respectively) compared with the optimum soil. On 'FLL', again, *Qp* and *Cb* were most restricted (-50% and -46% , respectively), whereas *Ls* and *Al* were the less negatively affected species (-10% and -12% respectively) compared with the optimum soil. The species *Al*, *Kp*, *Ls*, and *Oc* showed the same growth patterns found for their DBH growth, and also for their shoot growth (Figure 4b). The remaining species responded differently in terms of shoot growth compared with DBH growth. Across all species, tree shoot growth

on ‘Sand’ and ‘FLL’ was, on average, -50% and -18% , respectively, lower than that on the optimum planting soil. On ‘Sand’, *Qp* was, by far, the most restricted (-72%), whereas *Gt* was the less negatively affected species (-27%) compared with the optimum soil. On ‘FLL’, again, *Qp* was most restricted in terms of growth (-42%) compared with the optimum soil, whereas *Oc*, *Al*, *Kp*, *Ls*, *Qc*, and *Tc* were not significantly affected.

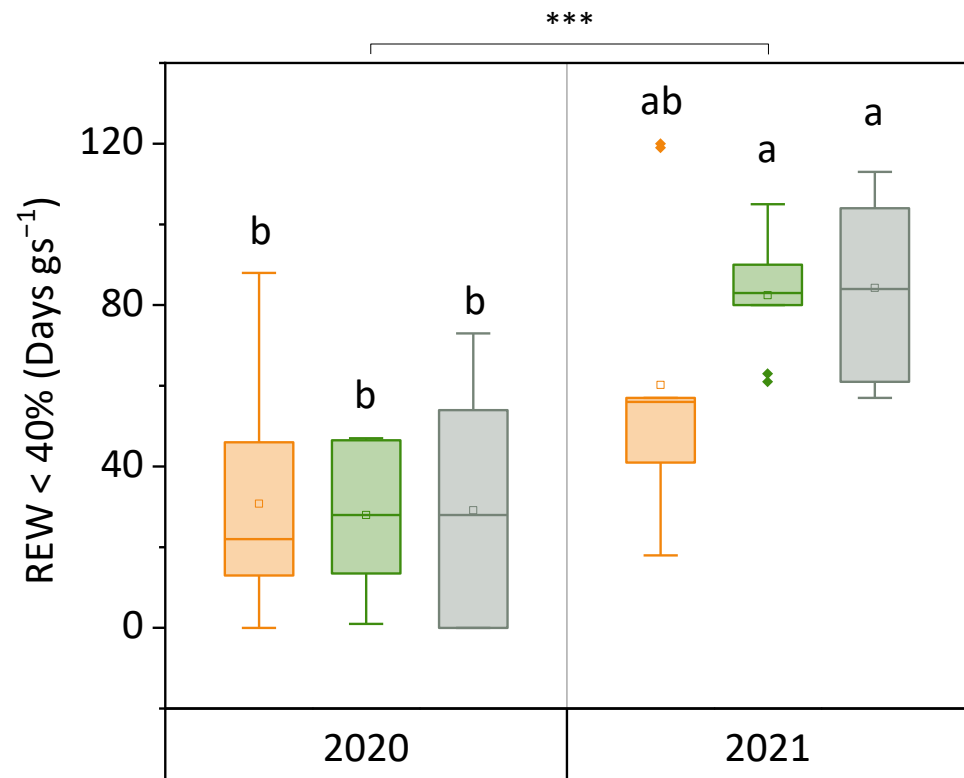


Figure 3. Sum of the number of days with REW < 40% (0–100 cm depth) during the growing season (gs) as a mean of the years 2020 and 2021 in the three planting soils ‘Sand’ (orange), ‘FLL’ (green), and ‘Loamy Silt’ (grey). Statistical analyses were performed by using a two-way ANOVA. Boxes with the same letters indicate no significant differences between the substrates at the $p \leq 0.05$ level. *** indicates significant differences between the years at the $p \leq 0.001$ level. Mean comparisons were performed by Tukey post hoc comparisons.

The assessed vitality scores of the years 2020 and 2021 were, across all species, the highest (i.e., lowered vitality) for the trees growing on ‘Sand’ (Table 3). In both years, *Al* and *Qp* had, on average, the highest values on ‘Sand’, whereas *Tc* had the lowest, which was also true for ‘FLL’ and ‘Loamy Silt’. The vitality scores of trees growing on ‘FLL’ and ‘Loamy Silt’ were mostly < 2 . Only *Kp* showed values > 2 , which was, in particular, striking for these trees growing in the optimum soil. We also noticed high vitality values for two individuals of *Qc* growing on the optimum soil, which was expressed by the elevated SD (Table 3).

Intra-annual stem diameter measurements for eight tree species (except for *Kp*) in ‘Sand’ showed a high variation of net growth (Figure 5). Growth onset was, on average, at the beginning of June and ceased, on average, at the beginning of August. During phases with REW < 40%, the daily stem diameter variations were pronounced with amplitudes varying evidently between species—they were weak in *Gs*, *Oc*, and *Qc*, and strong in *Tc* and *Ls*. The tree water deficit (TWD) is defined to occur when the maximum precedent stem diameter is greater than the maximum stem diameter of the actual day. Overall, the TWD was only weakly expressed ($< 120 \mu\text{m d}^{-1}$) and occurred for individuals of almost all species when REW < 40% (data not displayed). However, the TWD during the drought phases was most pronounced for *Al* and *Ls*, with single trees reaching maximum values

of 1130 and 627 $\mu\text{m d}^{-1}$, respectively. Single variable correlations were used to test the impact of the environmental variables REW at 0–35 cm and 0–100 cm, precipitation, and VPD on the tree species growth reactions using the weekly means of relative stem diameter increment (SDI) and the maximum daily shrinkage of the stem diameter (mds). The SDI of all trees investigated, except for *Qc*, was positively correlated with REW at least on the depth level ($p \leq 0.05$), rather than with precipitation or VPD (Table 4). SDI showed the strongest correlations (Spearman's $R > 0.6$) with REW for the species *Oc*, *Gt*, and *Ls*. The correlations of SDI and REW in 0–35 cm were, for *Gt* and *Al*, more significant than the correlations at 0–100 cm, whereas the growth of *Qp* and *Cb* was correlated more significant with REW 0–100 cm. Mds was correlated with both the soil water status and VPD. Mds and REW at both depth levels were positively correlated in all investigated species ($p \leq 0.001$), with the strongest correlations (Spearman's $R > 0.6$) for *Tc*, *Qc*, *Cb*, and *Al*. VPD was significantly negatively correlated with mds in all species ($p \leq 0.001$), except for *Gt* ($p > 0.1$) (Table 4).

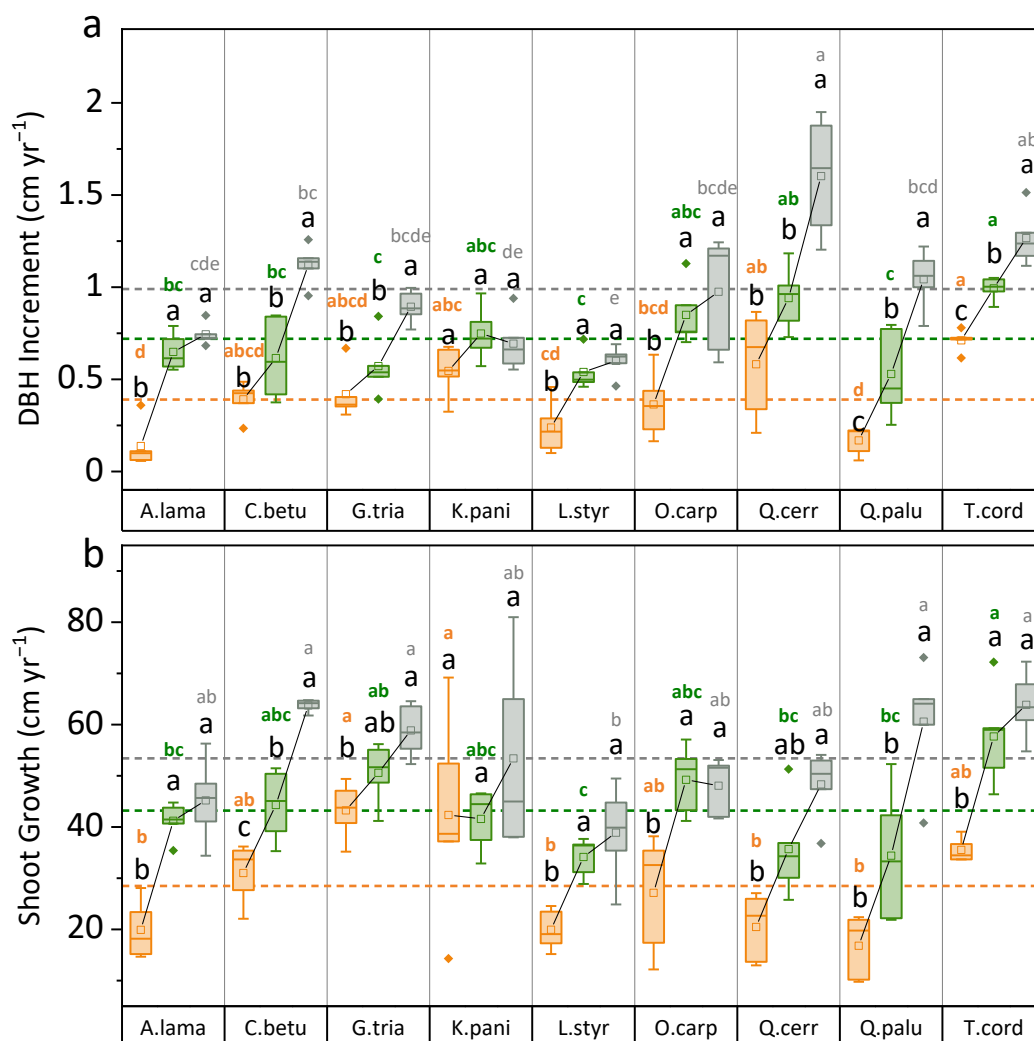


Figure 4. (a) Boxplots of annual DBH growth and (b) annual shoot growth of all nine tree species and as a mean of the years 2020–2021. Colored dashed lines show the mean growth across all species for the three planting soils ‘Sand’ (orange), ‘FLL’ (green), and ‘Loamy Silt’ (grey). Statistical analyses were performed by using a one-way ANOVA. Boxes with the same letters (black) indicate no significant differences at the $p \leq 0.05$ level within a species between the planting soils. Boxes with the same letters (see color assignment above) indicate no significant differences at the $p \leq 0.05$ level within a planting soil between the species. Mean comparisons were performed by Tukey post hoc comparisons.

Table 3. Tree vitality score assessed by visual inspections of the tree crowns in September 2020 and 2021. Values, ranked from 1 (vital) to 5 (strongly impaired), are presented as the means \pm SD for each species \times planting soil combination ($n = 5$).

Tree Species ‘Cultivar’	Vitality Score ¹					
	‘Sand’		‘FLL’		‘Loamy Silt’	
	2020	2021	2020	2021	2020	2021
<i>Tilia cordata</i> ‘Greenspire’	1.6 \pm 0.9	1.4 \pm 0.5	1.0 \pm 0.0	1.0 \pm 0.0	1.0 \pm 0.0	1.0 \pm 0.0
<i>Quercus cerris</i>	2.2 \pm 0.4	2.4 \pm 0.5	1.4 \pm 0.5	1.2 \pm 0.4	1.6 \pm 0.9	1.8 \pm 0.8
<i>Quercus palustris</i>	2.8 \pm 0.4	2.8 \pm 0.4	1.6 \pm 0.5	1.4 \pm 0.5	1.0 \pm 0.0	1.6 \pm 0.5
<i>Carpinus betulus</i> ‘Lucas’	2.2 \pm 0.4	1.8 \pm 0.4	1.8 \pm 0.4	1.2 \pm 0.4	1.2 \pm 0.4	1.0 \pm 0.0
<i>Ostrya carpinifolia</i>	2.6 \pm 0.5	2.2 \pm 0.8	1.8 \pm 0.4	1.8 \pm 0.4	1.2 \pm 0.4	1.2 \pm 0.4
<i>Gleditsia triacanthos</i> ‘Skyline’	2.4 \pm 0.5	1.6 \pm 0.5	2.2 \pm 0.4	1.6 \pm 0.5	1.2 \pm 0.4	1.0 \pm 0.0
<i>Liquidambar styraciflua</i>	2.2 \pm 0.4	2.0 \pm 0.0	1.0 \pm 0.0	1.0 \pm 0.0	1.2 \pm 0.4	1.2 \pm 0.4
<i>Amelanchier lamarckii</i>	3.0 \pm 1.0	3.6 \pm 0.9	1.6 \pm 0.5	1.6 \pm 0.5	1.4 \pm 0.5	1.0 \pm 0.0
<i>Koelreuteria paniculata</i>	2.4 \pm 0.9	2.8 \pm 0.8	2.4 \pm 0.9	2.0 \pm 0.7	2.4 \pm 1.1	3.2 \pm 1.5

¹ According to vitality assessment procedure from GALK = Deutsche Gartenamtsleiterkonferenz (GALK e.V.; German Garden Agency Directors Conference).

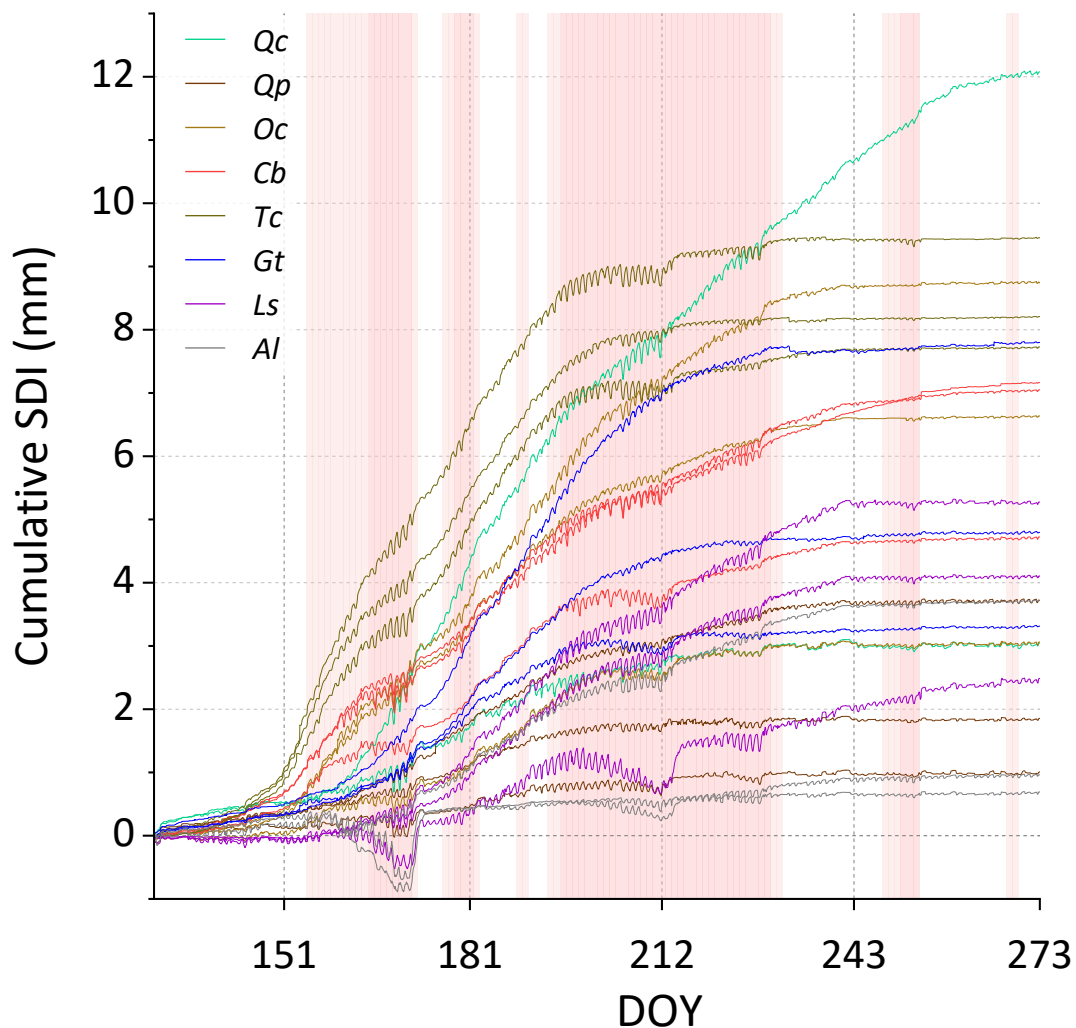


Figure 5. Cumulative stem diameter increment (SDI) of eight tree species grown in ‘Sand’ during the growing season of 2021. Reddish areas indicate phases when REW was $<40\%$ (light red: 0–35 cm; dark red: 0–100 cm).

Table 4. Spearman correlation coefficients[®] for the correlation of the relative stem diameter increment as weekly means (SDI; $n = 20$ data points per individual tree) and maximum daily shrinkage (mds; $n = 173$ data points per individual tree) of the stem diameter with the hydrological and climatological variables REW (relative extractable water), p (precipitation), and VPD (vapor pressure deficit) in eight species. Investigated period is defined according to the species-specific growing season length (Table 3)).

Weekly SDI	n	REW _{0–35 cm}	REW _{0–100 cm}	p	VPD
<i>Tilia cordata</i> ‘Greenspire’	3	0.43 **	0.53 **	ns	ns
<i>Quercus cerris</i>	2	ns	ns	ns	ns
<i>Quercus palustris</i>	3	0.42	0.45 ***	0.43	−0.41
<i>Carpinus betulus</i> ‘Lucas’	3	0.32	0.51 **	ns	ns
<i>Ostrya carpinifolia</i>	3	0.69 ***	0.85 ***	0.53 **	ns
<i>Gleditsia triacanthos</i> ‘Skyline’	3	0.64 ***	0.37	ns	ns
<i>Liquidambar styraciflua</i>	3	0.61 ***	0.73 ***	ns	ns
<i>Amelanchier lamarckii</i>	3	0.44 **	ns	0.38 **	ns
mds					
<i>Tilia cordata</i> ‘Greenspire’	3	0.67 ***	0.72 ***	0.23 **	−0.42 ***
<i>Quercus cerris</i>	2	0.6 ***	0.64 ***	ns	−0.57 ***
<i>Quercus palustris</i>	3	0.47 ***	0.48 ***	ns	−0.43 ***
<i>Carpinus betulus</i> ‘Lucas’	3	0.67 ***	0.53 ***	0.16 **	−0.38 ***
<i>Ostrya carpinifolia</i>	3	0.35 ***	0.4 ***	ns	−0.49 ***
<i>Gleditsia triacanthos</i> ‘Skyline’	3	0.34 ***	0.39 ***	ns	ns
<i>Liquidambar styraciflua</i>	3	0.6 ***	0.42 ***	0.19 **	−0.4 ***
<i>Amelanchier lamarckii</i>	3	0.63 ***	0.43 ***	0.26 **	−0.51 ***

Significance levels: ** $p \leq 0,01$; *** $p \leq 0,001$; ns = not significant.

4. Discussion

4.1. Substrate Characteristics

New street trees are often planted in artificial sandy-textured soil [5,33] or specific load-bearing substrates to resist compaction [23]. Up to now, these substrates were not well characterized in terms of soil hydrological properties [59], and it was unclear how the growth and vitality of specific tree species respond to the individual substrate conditions [9]. We used an experimental field setup with nine selected tree species and two urban tree sites representing planting soils to investigate this response under controlled field conditions.

Soil water availability is the most important parameter controlling tree growth [60–62]. With 10%, the plant available water capacity (PAWC) of ‘FLL’ was within the range reported for similar technical substrates (7–11%) [63] and exceeded the PAWC of ‘Sand’ (6%). ‘Loamy Silt’ had more than twice the amount of plant available water, mainly stored in the medium-sized pores of the dominating silt grains (Figure 1). As expectable, under field conditions, the REW in ‘Sand’ and ‘FLL’ was reduced sufficiently and faster than that in the optimum soil with the beginning of the growing season. However, regarding the seasonal average, no difference between the REW negatively exceeding the threshold value of 40% in the artificial soils and ‘Loamy Silt’ was visible (Figure 3). We assume that the different abilities to transport water caused this finding for the three planting soils. Precipitation water infiltrated the artificial soils faster and more effectively due to the higher infiltration capacity (IC), replenishing the PAWC, particularly at the 10 cm and 35 cm depths regularly. On the other hand, we assumed trees growing in the optimal soil to exploit the soil water stored more effectively, particularly at low soil water potentials, regardless of the absolutely higher quantity. This is reflected by the different hydraulic conductivities of the substrates during the process of drying (Figure 1b).

The large proportion of medium and fine pores in the total pore system of ‘Loamy Silt’ caused, under moist conditions ($<pF$ 1.8), slower water transport, but that under unsaturated conditions ($>pF$ 1.8–4.2) was almost constant. Compared to the ‘Sand’ and ‘FLL’, where large pores became quickly nonconductive with increasing soil water potential [64],

a higher amount of water was thus quantitatively available to the trees in 'Loamy Silt'. While the tree roots in the 'Loamy Silt' could be resupplied with soil water with almost no restriction, the development of dry zones around the tree roots [65], causing hydraulically disconnection from surrounding wet soil, was most likely the limiting factor for water supply in sandy and coarse porous soils, causing stomatal closure [66] and thus reduced water consumption. Hence, the drought stress avoidance strategies of trees relying on reducing the plant water potential (anisohydric reaction type) were likely to be not successful in sandy or coarsely porous artificial soils [67]. In order to tap further soil water, a tree able to adapt to sandy and coarse porous soils must invest in the production of fine roots that grow towards available water to bypass dry soil patches. Most likely, the exchange of soil water between the SWP sensor and soil is also affected in a comparative way. This resulted in wide standard deviations of the mean REW in 'Sand' and 'FLL' (Figure 2), suggesting that sufficient soil drying was only detected by sensors close to roots. Thus, a high sensor density would be needed to capture the spatial heterogeneity of the soil water distribution within sandy and coarse porous soils.

Overall, the seasonal water stress conditions determined by using the REW threshold value reported for forests [52] have been comparatively low [14,52,68] (Figure 3). In addition to the explanations mentioned, this may have resulted from an underdeveloped root:shoot ratio within three years after transplanting and regular and intense soil water replenishment from precipitation. The latter, however, would have been lower under actual urban site conditions due to sealing with impermeable pavements and soil compaction. Therefore, the use of rain-out shelters would have been necessary to simulate prolonged drought situations, as used by [41].

4.2. Tree Growth Analysis

So far, data regarding species-specific belowground requirements generated from growth response to ensure the establishment, initial growth, and long-term survival of young street trees in urban environments are scarce. The second- and third-season growth data of the trees planted in artificial soils were in the range of those of other studies for DBH- [24,25,69–71] and shoot growth [32]. In the first growing season, DBH- and shoot growth were similar among species, being low in all soils compared with those in the following years (Figure S3). This growth depression in the first year is in accordance with the finding of [28] that trees need time to recover from a transplanting shock (i.e., reestablishing the root:shoot ratio) and initially mainly profit from the uniform root ball soil conditions and irrigation [19]. This nexus is supported by our observation of high water consumption in the root ball and low consumption in the planting soils at all depths (Figure 2). In the second and third growing seasons, the growth of all species was constrained on the artificial soils compared with the optimal soil [9,24,72]. This is contrary to the findings of [25,29], who reported higher tree growth in the structural planting soils of 1.3–3.2 cm yr⁻¹ DBH (*Quercus bicolor*, *Quercus phellos*, and *Pyrus calleryana* 'Chanticleer'), compared with 0.3–0.6 cm yr⁻¹ in the artificial soils in our study. In particular, these authors found higher or equal growth of trees in structural soils compared with trees in tree lawns. However, data regarding the soil properties and soil characteristics (i.e., texture, organic matter content, bulk density) are not available and due to the smaller planting pit dimensions and multiple urban environmental constraints in these in situ studies; a comparison of the results with our study should be conducted with caution. Furthermore, it is likely that tree roots developed in the whole planting pit and extended into the surrounding soil a few years after planting [14,73]. This was supported by random excavations at the edges of the planting pits at the end of the third growing season, by the gradual reduction of REW down to 100 cm depth in all substrates until 2021 (Figure 2), and by the elevated growth of trees in 'Sand' and 'FLL' in 2021 compared with that in 2020 (Figure S3). As opposed to our experimental site where natural 'Loamy Silt' surrounded the planting pits, in urban settings, a growth decrease would be most likely when tree roots extend into the surrounding soils comparable to 'Sand' [1,5]. We, therefore, assume that a smaller planting

pit and thus an earlier extension of roots into the surrounding soil, when possible would also decrease tree growth and would make long-term comparison between soil conditions inappropriate [29].

Little attention has been paid to the morphological and physiological responses of tree species to artificial urban soils [9,71]. Across all substrates, we found the strongest annual DBH growth rates for *Qc* and the lowest for *Ls*, and the strongest annual shoot growth for *Tc* and the lowest also for *Ls* (Figure 4a,b). The response of the investigated tree species was different [9,24].

Although *Tc* invested strongly in stem growth, even under the unfavorable soil conditions of 'Sand' and 'FLL', the vitality scores, particularly in 'Sand', indicated apparently good performance also in the third growing season. This outcome is in contrast to the findings from [41], where the isohydric *Tc* [74] was highly affected by water scarcity, showing early leaf senescence. Since, in that study, extreme drought situations were caused on sandy loam by using rain-out shelters, it seems plausible that *Tc* is unable to extract water from drying, fine-grained soils [75]. In the sandy and coarse porous artificial soils used in our study, *Tc* showed, contrary to [76], no growth reduction during the phases of low REW in the 'Sand' and, despite the high mds, almost no TWD (Figure 5). These observations indicate that *Tc*, at least the cultivar 'Greenspire', is seemingly well-adapted to artificial urban soils characterized by low hydraulic conductivity. We hypothesize that this adaptation comes with a drought strategy that does not rely on increasing the suction power of roots, but on growing roots towards the water. This hypothetical reaction pattern of *Tc* in urban soils and the long-term effect on the C-balance should be investigated further in order to reliably assess the mortality risk in urban environments under climate change.

Contrary to *Tc*, the overall growth rates of *Ls* were very low [71] (Figure 4). However, compared with the optimal soil, the DBH and shoot growth were equal or above average for all species in 'Sand' and 'FLL', respectively, and trees in 'FLL' maintained the best possible vitality score (Figure 5). During the growing season, the growth of *Ls* was strongly correlated with REW (Table 4), indicating that investment in above-ground biomass was reduced during phases of low REW. This suggests that, under drought conditions, assimilated and stored C had not been allocated to growth, but rather to mechanisms successfully coping with drought stress. This is in accordance with [71], who found the lowest annual mortality rates for *Ls* among 10 species investigated in a subtropical city in Florida, USA. This indicates, in accordance with our results, that *Ls* is capable of withstanding dry soils [77] and that, in general, high growth rates in urban soils alone are not a categorical identifier for the adaptability of a tree species to the harsh urban environment under future climates.

In contrast to 'FLL', the growth of *Al* in 'Sand' was different to that of *Ls* and almost the lowest of all species, while simultaneously being obviously non-vigorous (Table 3). *Al* was the only species that grew less in 2021 compared with 2020 (data not shown) and where SDI and mds were correlated mainly with REW in the upper soil compartment (Table 4). Thus, we assume that *Al* was neither unable to develop a sufficient, deep-rooting system within the planting pit, nor expand its roots into the favorable surrounding soil.

The *Quercus* species *Qc* and *Qp* showed overall high growth rates in the optimal soil. The DBH growth of *Qc* in the artificial soils was higher than the average of all species. The tree growth in 'Sand' was particularly variable, which suggests different abilities of individuals to react to coarse-textured soil with a low OM content within the species. *Qp*, on the other hand, experienced the largest growth inhibition of all tree species in sandy soils compared with the optimal soil. Currently, *Qp* is, among the studied species, one of the most abundant species in Hamburg's street tree population. However, it appears to be highly reactive to poor soil conditions. Furthermore, care should be taken that soils in *Qp* planting sites have pH values < 6.5 to prevent leaf chlorosis [78], which was visible for the trees in the 'Sand', but not in 'FLL' (Tables 1 and 3), whereas soil compaction and water logging might play minor roles in *Qp* growth [79]. Regardless of the constraints in the artificial soils, heavy precipitation caused prolonged waterlogging conditions during June 2020 and affected the 'Loamy Silt' trees of *Qc* in terms of vitality and *Kp* in terms

of growth and vitality (Table 3). This suggests that both tree species need well-aerated, non-compacted soils at sites that do not tend toward waterlogging [80]. Despite the high variability in shoot growth in ‘Sand’, the DBH growth of *Kp* was comparatively high in the artificial soils. We assumed that *Kp* combined the ability of both, lowering its water potential in fine-grained soils [67], and growing with roots toward the water in coarsely textured and porous soils. However, the comparatively poor vitality of *Kp* in the artificial soils may have also resulted from the low REW conditions during mid-June 2021, since *Kp* is reported to be very sensitive to early growing season drought [67].

The DBH growth rates of *Cb* and *Oc* in the optimal soil were higher than those reported by [81] with similar soil properties. Compared with the optimal soil, *Cb* and *Oc* showed, in our study, similar growth reduction between 60% and 65% in ‘Sand’; [81] also reported similar growth reduction for treatment plots where precipitation water infiltration was prevented by rain-out shelters; however, growth was reduced by up to 79% compared with the control plot. Contrary to growth in ‘Sand’, *Oc* showed in ‘FLL’ substantially higher growth than the more vital *Cb* compared with the optimum soil; [82] concluded that both species had the lowest resistance of growth under drought conditions in fine-grained soils. However, we found both species to be not affected above average in artificial planting soils, despite the low PAWC.

Considering that *Gt* had above-average growth and the lowest mds rates in ‘Sand’, it seems most likely that *Gt* is suitable for harsh urban street tree sites and persists under water-stress conditions [83]. However, the strong and significant correlation of growth with REW at 0–35 cm suggests that the roots are more likely to grow near the surface. This can be problematic and requires further investigation.

Under the slightly dry, but less extreme, meteorological conditions in terms of air/soil temperatures and relative humidity compared with inner cities, the studied trees established within the study period of three years. For the trees, the selected artificial planting soils were thus sufficient for survival in the short term. In the long term, it is most likely that the formation of above ground biomass, the assimilation of carbohydrate reserves, and the provision of ecosystem services may be limited. However, at actual urban street tree sites, trees will face additional constraints affecting tree growth. Further investigations are necessary to understand the mechanistic adaptations of tree species in response to planting soils (permanent stress) and periods of low REW (temporal stress), particularly regarding patterns of carbon allocation under permanent and temporal soil water stress [36]. Our investigations provide a first insight into growth-limiting conditions and tree species-specific differences triggered by ‘artificial soils’ with different hydrological properties, and the experimental design was proven successful and should be continued in the future. In addition, other relevant tree species not considered in this study should be investigated for their growth behavior under soil conditions representative of urban street sites. Such tree species could include *Robinia pseudoacacia* [84,85], *Quercus robur* [86,87], or *Platanus* spp. [88], which have shown properties suitable for urban road-side conditions.

5. Conclusions

We showed that sandy-textured urban planting soils—one representing structural pit filling and one representing local surrounding soil conditions—have low plant available water capacities and were restricted in terms of hydraulic conductivity when the soil dries. Thus, when the soil water potential decreased and the pore space became non-conductive due to the high percentage of air-filled pores, the amount of water quantitatively available for the tree decreased. Therefore, trees that invest more in the fine root system to bypass soil non-conductivity (e.g., *Tilia cordata* ‘Greenspire’ and *Liquidambar styraciflua*) might be more successful in sandy and coarse porous soils than trees that lower their water potential, which might be successful in fine-textured drying soils (e.g., *Koeleruteria paniculata*, *Quercus cerris*; [67]). However, the tree growth of all species on the artificial urban soils was significantly constrained. The selected artificial planting soils were sufficient to survive, but most likely did not encourage the trees to build up above ground biomass, to assimilate

carbohydrate reserves, or to provide effective ecosystem services in the long term. Thus, improving the hydrological properties of planting soils at street tree sites is crucial to allow newly planted trees to grow and thrive.

Supplementary Materials: The following supporting information can be downloaded at: <https://www.mdpi.com/article/10.3390/f13060936/s1> (accessed on). Figure S1: Spatial distribution of planting pits, treatment and control plantation soils, and tree species in a 4 × 35 grid. Figure S2: View of the experimental site in the western direction in June 2019. The three planting soils are clearly visible (light = ‘Sand’; dark = ‘FLL’; and brown = ‘Loamy Silt’). Watering bags were removed after 2019. Figure S3: Annual DBH and shoot growth in each investigated year as a mean of all species ($n = 9$) in the planting soils ($n = 3$). Statistical analyses were performed by using a one-way ANOVA. Boxes with the same letters indicate no significant differences at the $p \leq 0.05$ level. Mean comparisons were performed by Tukey post hoc comparisons.

Author Contributions: Conceptualization, A.S., C.R. and A.E.; methodology, A.S.; software, A.S.; validation, J.N.B., C.R. and A.E.; formal analysis, A.S.; investigation, A.S.; resources, A.E.; data curation, J.N.B.; writing—original draft preparation, A.S.; writing—review and editing, J.N.B., C.R., and A.E.; visualization, A.S.; supervision, C.R. and A.E.; project administration, A.E.; funding acquisition, A.E. All authors have read and agreed to the published version of the manuscript.

Funding: This research was funded by the Federal Ministry for the Environment, Nature Conservation, Nuclear Safety and Consumer Protection (BMUV), Zukunft-Umwelt-Gesellschaft (ZUG) GmbH, grant number 67DAS153A, as an initiative under DAS: Förderung von Maßnahmen zur Anpassung an den Klimawandel, and by Deutsche Forschungsgemeinschaft (DFG, German Research Foundation) under Germany’s Excellence Strategy—EXC 2037 “CLICCS—Climate, Climatic Change, and Society” Project Number: 390683824—contribution to the Center for Earth System Research and Sustainability (CEN) of Universität Hamburg. Further financial support was given by Freie und Hansestadt Hamburg FHH, and Behörde für Umwelt, Klima, Energie und Agrarwirtschaft (BUKEA).

Institutional Review Board Statement: Not applicable.

Informed Consent Statement: Not applicable.

Acknowledgments: Many thanks to Volker Kleinschmidt for various sensor installations and his professional technical support during planning and measurements. We would like to thank Baumschule Lorenz von Ehren GmbH & Co. KG for providing their ground and the trees, and for their manifold support to realize the experimental site. Many thanks also to K + E (Kompost und Erden GmbH) for providing the structural planting soil and to Annette Wagner and Torsten Melzer from BUKEA (Free and Hanseatic City of Hamburg, Department for the Environment, Climate, Energy and Agriculture) for their cooperation, data support, and tree vitality assessment during 2020 and 2021. We would also like to thank Gerhard Doobe from GALK e.V. AK Stadtbäume and Alexander Gröngröft for fruitful discussions.

Conflicts of Interest: The authors declare no conflict of interest. The funders had no role in the design of the study; in the collection, analyses, or interpretation of data; in the writing of the manuscript, or in the decision to publish the results.

References

1. Jim, C.Y. Urban soil characteristics and limitations for landscape planting in Hong Kong. *Landscape Urban Plan.* **1998**, *40*, 235–249. [[CrossRef](#)]
2. Clark, J.R.; Kjelgren, R. Water as a limiting factor in the development of urban trees. *J. Arboric.* **1990**, *16*, 203–209. [[CrossRef](#)]
3. Craul, P.J. A description of urban soils and their desired characteristics. *J. Arboric.* **1985**, *11*, 330–339.
4. Wessolek, G.; Kluge, B.; Toland, A.; Nehls, T.; Klingelmann, E.; Rim, Y.N.; Mekiffer, B.; Trinks, S. Urban Soils in the Vadose Zone. In *Wilfried Endlicher (Hg.): Perspectives in Urban Ecology*; Springer: Berlin/Heidelberg, Germany, 2011.
5. Jim, C.Y.; Ng, Y.Y. Porosity of roadside soil as indicator of edaphic quality for tree planting. *Ecol. Eng.* **2018**, *120*, 364–374. [[CrossRef](#)]
6. Armson, D.; Stringer, P.; Ennos, A.R. The effect of street trees and amenity grass on urban surface water runoff in Manchester, UK. *Urban For. Urban Green.* **2013**, *12*, 282–286. [[CrossRef](#)]
7. Morgenroth, J.; Buchan, G.; Scharenbroch, B.C. Belowground effects of porous pavements—Soil moisture and chemical properties. *Ecol. Eng.* **2013**, *51*, 221–228. [[CrossRef](#)]

8. Cermák, J.; Hruska, J.; Martinková, M.; Prax, A. Urban tree root systems and their survival near houses analyzed using ground penetrating radar and sap flow techniques. *Plant Soil* **2000**, *219*, 103–116. [[CrossRef](#)]
9. Pregitzer, C.C.; Sonti, N.F.; Hallett, R.A. Variability in Urban Soils Influences the Health and Growth of Native Tree Seedlings. *Ecol. Restor.* **2016**, *34*, 106–116. [[CrossRef](#)]
10. Roetzer, T.; Wittenzeller, M.; Haeckel, H.; Nekovar, J. Phenology in central Europe—differences and trends of spring phenophases in urban and rural areas. *Int. J. Biometeorol.* **2000**, *44*, 60–66. [[CrossRef](#)]
11. Schnabel, F.; Purrucker, S.; Schmitt, L.; Engelmann, R.A.; Kahl, A.; Richter, R.; Seele-Dilbat, C.; Skiadaresis, G.; Wirth, C. Cumulative growth and stress responses to the 2018–2019 drought in a European floodplain forest. *Glob. Chang. Biol.* **2021**, *28*, 1870–1883. [[CrossRef](#)]
12. Schuldt, B.; Buras, A.; Arend, M.; Vitasse, Y.; Beierkuhnlein, C.; Damm, A.; Gharun, M.; Grams, T.E.E.; Hauck, M.; Hajek, P.; et al. A first assessment of the impact of the extreme 2018 summer drought on Central European forests. *Basic Appl. Ecol.* **2020**, *45*, 86–103. [[CrossRef](#)]
13. Hartmann, H. Will a 385 million year-struggle for light become a struggle for water and for carbon?—How trees may cope with more frequent climate change-type drought events. *Glob. Change Biol.* **2011**, *17*, 642–655. [[CrossRef](#)]
14. Schütt, A.; Becker, J.N.; Schaaf-Titel, S.; Groengroeft, A.; Eschenbach, A. Soil water stress at young urban street-tree sites in response to meteorology and site parameters. *Urban For. Urban Green.* *in review*.
15. Schlünzen, K.H.; Hoffmann, P.; Rosenhagen, G.; Riecke, W. Long-term changes and regional differences in temperature and precipitation in the metropolitan area of Hamburg. *Int. J. Climatol.* **2010**, *30*, 1121–1136. [[CrossRef](#)]
16. Quigley, M.F. Street trees and rural conspecifics: Will long-lived trees reach full size in urban conditions? *Urban Ecosyst.* **2004**, *7*, 29–39. [[CrossRef](#)]
17. Gillner, S.; Vogt, J.; Roloff, A. Climatic response and impacts of drought on oaks at urban and forest sites. *Urban For. Urban Green.* **2013**, *12*, 597–605. [[CrossRef](#)]
18. Pretzsch, H.; Biber, P.; Uhl, E.; Dahlhausen, J.; Schütze, G.; Perkins, D.; Rötzer, T.; Caldentey, J.; Koike, T.; Van Con, T.; et al. Climate change accelerates growth of urban trees in metropolises worldwide. *Sci. Rep.* **2017**, *7*, 15403. [[CrossRef](#)]
19. Watson, W.T. Influence of Tree Size on Transplant Establishment and Growth. *Horttech* **2005**, *15*, 118–122. [[CrossRef](#)]
20. Roman, L.A.; Scatena, F.N. Street tree survival rates: Meta-analysis of previous studies and application to a field survey in Philadelphia, PA, USA. *Urban For. Urban Green.* **2011**, *10*, 269–274. [[CrossRef](#)]
21. Roman, L.A.; Battles, J.J.; McBride, J.R. The balance of planting and mortality in a street tree population. *Urban Ecosyst.* **2014**, *17*, 387–404. [[CrossRef](#)]
22. Nowak, D.J.; Kuroda, M.; Crane, D.E. Tree mortality rates and tree population projections in Baltimore, Maryland, USA. *Urban For. Urban Green.* **2004**, *2*, 139–147. [[CrossRef](#)]
23. Grabosky, J.; Bassuk, N. Testing of structural urban tree soil materials for Use under Pavement to Increase Street Tree Rooting Volumes. *J. Arboric.* **1996**, *22*, 255–263. [[CrossRef](#)]
24. Smiley, E.T.; Calfee, L.; Fraedrich, B.R.; Smiley, E.J. Comparison of Structural and Noncompacted Soils for Trees Surrounded by Pavement. *Arboric. Urban For.* **2006**, *32*, 164–169. [[CrossRef](#)]
25. Rahman, M.A.; Smith, J.G.; Stringer, P.; Ennos, A.R. Effect of rooting conditions on the growth and cooling ability of *Pyrus calleryana*. *Urban For. Urban Green.* **2011**, *10*, 185–192. [[CrossRef](#)]
26. Grabosky, J. Establishing a common method to compare soil systems designed for both tree growth and pavement support. Research Note. *Soil Sci.* **2015**, *180*, 207–213. [[CrossRef](#)]
27. Bühler, O.; Ingerslev, M.; Skov, S.; Schou, E.; Thomsen, I.M.; Nielsen, C.N.; Kristoffersen, P. Tree development in structural soil—An empirical below-ground in-situ study of urban trees in Copenhagen, Denmark. *Plant Soil* **2017**, *413*, 29–44. [[CrossRef](#)]
28. Bretzel, F.; Vannucchi, F.; Pini, R.; Scatena, M.; Marradi, A.; Cinelli, F. Use of coarse substrate to increase the rate of water infiltration and the bearing capacity in tree plantings. *Ecol. Eng.* **2020**, *148*, 105798. [[CrossRef](#)]
29. Grabosky, J.; Bassuk, N. Seventeen years' growth of street trees in structural soil compared with a tree lawn in New York City. *Urban For. Urban Green.* **2016**, *16*, 103–109. [[CrossRef](#)]
30. FLL. Empfehlungen für Baumpflanzungen Teil 2. In *Standortvorbereitungen für Neuanpflanzungen; Pflanzgruben und Wurzelraumvergrößerung, Bauweisen und Substrate*; Forschungsgesellschaft Landschaftsentwicklung Landschaftsbau e.V. (FLL): Bonn, Germany, 2010.
31. Nielsen, C.N.; Bühler, O.; Kristoffersen, P. Soil water dynamics and growth of street and park trees. *Arboric. Urban For.* **2007**, *33*, 231–245. [[CrossRef](#)]
32. Riikonen, A.; Lindén, L.; Pulkkinen, M.; Nikinmaa, E. Post-transplant crown allometry and shoot growth of two species of street trees. *Urban For. Urban Green.* **2011**, *10*, 87–94. [[CrossRef](#)]
33. Schickhoff, U.; Eschenbach, A. Terrestrische und semiterrestrische Ökosysteme. In *Hans von Storch, Insa Meinke und Martin Claußen (Hg.): Hamburger Klimabericht—Wissen über Klima, Klimawandel und Auswirkungen in Hamburg und Norddeutschland*; Springer: Berlin/Heidelberg, Germany, 2018.
34. Somerville, P.D.; Farrell, C.; May, P.B.; Livesley, S.J. Tree water use strategies and soil type determine growth responses to biochar and compost organic amendments. *Soil Tillage Res.* **2019**, *192*, 12–21. [[CrossRef](#)]

35. Blackman, C.J.; Creek, D.; Maier, C.; Aspinwall, M.J.; Drake, J.E.; Pfautsch, S.; O'Grady, A.; Delzon, S.; E Medlyn, B.; Tissue, D.T.; et al. Drought response strategies and hydraulic traits contribute to mechanistic understanding of plant dry-down to hydraulic failure. *Tree Physiol.* **2019**, *39*, 910–924. [CrossRef] [PubMed]
36. Trugman, A.T.; Detto, M.; Bartlett, M.K.; Medvigy, D.; Anderegg, W.R.L.; Schwalm, C.; Schaffer, B.; Pacala, S.W. Tree carbon allocation explains forest drought-kill and recovery patterns. *Ecol. Lett.* **2018**, *21*, 1552–1560. [CrossRef] [PubMed]
37. Adams, H.D.; Zeppel, M.J.B.; Anderegg, W.R.L.; Hartmann, H.; Landhäusser, S.M.; Tissue, D.T.; Huxman, T.E.; Hudson, P.J.; Franz, T.E.; Allen, C.D.; et al. A multi-species synthesis of physiological mechanisms in drought-induced tree mortality. *Nat. Ecol. Evol.* **2017**, *1*, 1285–1291. [CrossRef]
38. Mitchell, P.J.; O'Grady, A.P.; Tissue, D.T.; Worledge, D.; Pinkard, E.A. Co-ordination of growth, gas exchange and hydraulics define the carbon safety margin in tree species with contrasting drought strategies. *Tree Physiol.* **2014**, *34*, 443–458. [CrossRef]
39. Roloff, A.; Korn, S.; Gillner, S. The Climate-Species-Matrix to select tree species for urban habitats considering climate change. *Urban For. Urban Green.* **2009**, *8*, 295–308. [CrossRef]
40. Böll, S.; Schönfeld, P.; Körber, K.; Herrmann, J.V. Stadtbäume unter Stress. Projekt »Stadtgrün 2021« untersucht Stadtbäume im Zeichen des Klimawandels. *LWF Aktuell* **2014**, *98*, 4–8.
41. Stratópoulos, L.M.F.; Zhang, C.; Häberle, K.-H.; Pauleit, S.; Duthweiler, S.; Pretzsch, H.; Rötzer, T. Effects of Drought on the Phenology, Growth, and Morphological Development of Three Urban Tree Species and Cultivars. *Sustainability* **2019**, *11*, 5117. [CrossRef]
42. Schönfeld, P. Klimabäume. Welche Arten können in Zukunft gepflanzt werden? *LWG Aktuell*. 2019. Available online: https://www.lwg.bayern.de/mam/cms06/landespflege/dateien/zukunft_klimabaeume.pdf (accessed on 15 March 2022).
43. DWD. CDC (Climate Data Center). Deutscher Wetterdienst. 2020. Available online: <https://www.dwd.de> (accessed on 15 March 2022).
44. Watson, G.W.; Hewitt, A.M.; Cusic, M.; Lo, M. The management of tree root systems in urban and suburban settings II. A Review of Strategies to Mitigate Human Impacts. *Arboric. Urban For.* **2014**, *40*, 249–271. [CrossRef]
45. Roloff, A. Aktualisierte KlimaArtenMatrix 2021 ("KLAM 2.0"). Unter Mitarbeit von Sten Gillner und Ulrich Pietzarka. In *Andreas Roloff (Hg.): Trockenstress bei Bäumen. Ursachen, Strategien, Praxis. Unter Mitarbeit von Anne Dreßler, Britt Kniesel, Doris Krabel, Liu Ming, Ulrich Pietzarka, Andreas Roloff und Lauritz Schrader*; Quelle & Meyer Verlag GmbH & Co.: Wiebelsheim, Germany, 2021; pp. 201–230.
46. Allen, K.S.; Harper, R.W.; Bayer, A.; Brazee, N.J. A review of nursery production systems and their influence on urban tree survival. *Urban For. Urban Green.* **2017**, *21*, 183–191. [CrossRef]
47. UMS GmbH. Manual HYPROP. UMS GmbH. Gmunder Str. 37, 81379 München, Germany (Version 2015-1). 2015. Available online: http://library.metergroup.com/Manuals/UMS/Hyprop_Manual.pdf (accessed on 25 February 2022).
48. Pertassek, T.; Peters, A.; Durner, W. *HYPROP-FIT Software User's Manual*, V. 3.0. Hg. v, UMS GmbH. Gmunder Str. 37, 81379: München, Germany. 2015. Available online: http://www.soil.tu-bs.de/download/downloads/reports/2015.Manual_HYPROP-FIT.pdf (accessed on 25 February 2022).
49. van Genuchten, M.T. A Closed-form Equation for Predicting the Hydraulic Conductivity of Unsaturated Soils. *Soil Sci. Soc. Am. J.* **1980**, *44*, 892–898. [CrossRef]
50. Shock, C.C.; Barnum, J.M.; Seddigh, M. Calibration of Watermark Soil Moisture Sensors for Irrigation Management. 1998. Available online: https://www.researchgate.net/profile/Clinton-Shock/publication/228762944_Calibration_of_W-ermark_Soil_Moisture_Sensors_for_Irrigation_Management/links/55ed971408ae3e12184819e7/Calibration-of-W-ermark-Soil-Moisture-Sensors-for-Irrigation-Management.pdf?_sg%5B0%5D=HUftqZa51n_ochZIOZEB02YVuEJmDUsBgvCjg5iiy4Sv_CbwSpvfGkQ8yis9DLhS7fHrHI0uGRK4hkLWwK9yWw.z_OgBYeZ6_vc09Hy93oOgqYnxbktt8rNEhCW_0wvFD4FD7NX7icVsJP4hfdPqVnKgnsjCJpB9gWmD-8mzsNqRw&_sg%5B1%5D=J7mKCVEDnOcsiBZC8HLO3AulvwVF5U-xR5w9gkJDwCG2IfsGI9bNH_KVfMxdLEFgW7AKUm2qQJ3gzGdN98zGopYvHUDdpSHGe6XLszU4x8D.z_OgBYeZ6_vc09Hy93oOgqYnxbktt8rNEhCW_0wvFD4FD7NX7icVsJP4hfdPqVnKgnsjCJpB9gWmD-8mzsNqRw&_iepl= (accessed on 14 February 2022).
51. Allen, R. *Calibration for the Watermark 200SS Soil Water Potential Sensor to Fit the 7-19-96—Calibration #3*||Table; University of Idaho: Kimberly, ID, USA, 2000.
52. Granier, A.; Reichstein, M.; Bréda, N.; Janssens, I.A.; Falge, E.; Ciais, P.; Grünwald, T.; Aubinet, M.; Berbigier, P.; Bernhofer, C.; et al. Evidence for soil water control on carbon and water dynamics in European forests during the extremely dry year: 2003. *Agric. For. Meteorol.* **2007**, *143*, 123–145. [CrossRef]
53. Granier, A.; Breda, N.; Biron, P.; Vilette, S. A lumped water balance model to evaluate duration and intensity of drought constraints in forest stands. *Ecol. Model.* **1999**, *116*, 269–283. [CrossRef]
54. R Core Team. *A Language and Environment for Statistical Computing*; R Foundation for Statistical Computing: Vienna, Austria, 2022.
55. Knüsel, S.; Peters, R.L.; Haeni, M.; Wilhelm, M.; Zweifel, R. Processing and Extraction of Seasonal Tree Physiological Parameters from Stem Radius Time Series. *Forests* **2021**, *12*, 765. [CrossRef]
56. Zweifel, R.; Haeni, M.; Buchmann, N.; Eugster, W. Are trees able to grow in periods of stem shrinkage? *New Phytol.* **2016**, *211*, 839–849. [CrossRef]
57. Köcher, P.; Horna, V.; Leuschner, C. Environmental control of daily stem growth patterns in five temperate broad-leaved tree species. *Tree Physiol.* **2012**, *32*, 1021–1032. [CrossRef]

58. Deslauriers, A.; Rossi, S.; Anfodillo, T. Dendrometer and intra-annual tree growth: What kind of information can be inferred? *Dendrochronologia* **2007**, *25*, 113–124. [[CrossRef](#)]
59. Yilmaz, D.; Cannavo, P.; Séré, G.; Vidal-Beaudet, L.; Legret, M.; Damas, O.; Peyneau, P.-E. Physical properties of structural soils containing waste materials to achieve urban greening. *J. Soils Sediments* **2018**, *18*, 442–455. [[CrossRef](#)]
60. Allen, C.D.; Macalady, A.K.; Chenchouni, H.; Bachelet, D.; McDowell, N.; Vennetier, M.; Kitzberger, T.; Rigling, A.; Breshears, D.D.; Hogg, E.H.; et al. A global overview of drought and heat-induced tree mortality reveals emerging climate change risks for forests. *For. Ecol. Manag.* **2010**, *259*, 660–684. [[CrossRef](#)]
61. Bréda, N.; Granier, A.; Barataud, F.; Moyne, C. Soil water dynamics in an oak stand. I. Soil moisture, water potentials and water uptake by roots. *Plant Soil* **1995**, *172*, 17–27. [[CrossRef](#)]
62. Puhlmann, H.; Schmidt-Walter, P.; Hartmann, P.; Meesenburg, H.; von Wilpert, K. Soil Water Budget and Drought Stress. In *Nicole Wellbrock und Andreas Bolte (Hg.): Status and Dynamics of Forests in Germany, Bd. 237*; Springer International Publishing (Ecological Studies): Cham, Switzerland, 2019; pp. 55–91.
63. Grabosky, J.; Haffner, E.; Bassuk, N. Plant available Moisture in Stone-soil Media for Use under pavement while allowing urban tree root growth. *Arboric. Urban For.* **2009**, *35*, 271–278. [[CrossRef](#)]
64. Li, K.I.; De Jong, R.; Coe, M.T.; Ramankutty, N. Root-Water-Uptake Based upon a New Water Stress Reduction and an Asymptotic Root Distribution Function. *Earth Interact.* **2006**, *10*, 1–14. [[CrossRef](#)]
65. Schulze, E.-D.; Beck, E.; Buchmann, N.; Clemens, S.; Müller-Hohenstein, K.; Scherer-Lorenzen, M. *Plant Ecology*; Springer: Berlin/Heidelberg, Germany, 2019.
66. Abdalla, M.; Carminati, A.; Cai, G.; Javaux, M.; Ahmed, M.A. Stomatal closure of tomato under drought is driven by an increase in soil–root hydraulic resistance. *Plant Cell Environ.* **2021**, *44*, 425–431. [[CrossRef](#)] [[PubMed](#)]
67. Sjöman, H.; Hirons, A.D.; Bassuk, N.L. Improving confidence in tree species selection for challenging urban sites: A role for leaf turgor loss. *Urban Ecosyst.* **2018**, *21*, 1171–1188. [[CrossRef](#)]
68. Schmidt-Walter, P.; Ahrends, B.; Mette, T.; Puhlmann, H.; Meesenburg, H. NFIWADS: The water budget, soil moisture, and drought stress indicator database for the German National Forest Inventory (NFI). *Ann. For. Sci.* **2019**, *76*, 39. [[CrossRef](#)]
69. Bühler, O.; Nielsen, C.N.; Kristoffersen, P. Growth and phenology of established *Tilia cordata* street trees in response to different irrigation regimes. *Arboric. Urban For.* **2006**, *32*, 3–9. [[CrossRef](#)]
70. Boukili, V.K.S.; Bebbler, D.P.; Mortimer, T.; Venicx, G.; Lefcourt, D.; Chandler, M.; Eisenberg, C. Assessing the performance of urban forest carbon sequestration models using direct measurements of tree growth. *Urban For. Urban Green.* **2017**, *24*, 212–221. [[CrossRef](#)]
71. Lawrence, A.B.; Escobedo, F.J.; Staudhammer, C.L.; Zipperer, W. Analyzing growth and mortality in a subtropical urban forest ecosystem. *Landsc. Urban Plan.* **2012**, *104*, 85–94. [[CrossRef](#)]
72. Loh, F.C.W.; Grabosky, J.C.; Bassuk, N.L. Growth response of *Ficus benjamina* to limited soil volume and soil dilution in a skeletal soil container study. *Urban For. Urban Green.* **2003**, *2*, 53–62. [[CrossRef](#)]
73. Krieter, M.; Malkus, A. *Untersuchungen zur Standortoptimierung von Straßenbäumen: Ergebnisse eines FLL-Pflanzversuches von Tilia Pallida in 14 Deutschen Städten*; FLL: Bonn, Germany, 1996.
74. Moser, A.; Rahman, M.A.; Pretzsch, H.; Pauleit, S.; Rötzer, T. Inter- and intraannual growth patterns of urban small-leaved lime (*Tilia cordata* mill.) at two public squares with contrasting microclimatic conditions. *Int. J. Biometeorol.* **2017**, *61*, 1095–1107. [[CrossRef](#)]
75. Gillner, S.; Korn, S.; Hofmann, M.; Roloff, A. Contrasting strategies for tree species to cope with heat and dry conditions at urban sites. *Urban Ecosyst.* **2017**, *20*, 853–865. [[CrossRef](#)]
76. Moser, A.; Rötzer, T.; Pauleit, S.; Pretzsch, H. The Urban Environment Can Modify Drought Stress of Small-Leaved Lime (*Tilia cordata* Mill.) and Black Locust (*Robinia pseudoacacia* L.). *Forests* **2016**, *7*, 71. [[CrossRef](#)]
77. Baraldi, R.; Przybysz, A.; Facini, O.; Pierdonà, L.; Carriero, G.; Bertazza, G.; Neri, L. Impact of Drought and Salinity on Sweetgum Tree (*Liquidambar styraciflua* L.): Understanding Tree Ecophysiological Responses in the Urban Context. *Forests* **2019**, *10*, 1032. [[CrossRef](#)]
78. Watson, G.W.; Himelick, E.B. Effects of soil pH, root density and tree growth regulator treatments on pin oak chlorosis. *J. Arboric.* **2004**, *30*, 172–178. [[CrossRef](#)]
79. Watson, G.W.; Kelsey, P. The impact of soil compaction on soil aeration and fine root density of *Quercus palustris*. *Urban For. Urban Green.* **2006**, *4*, 69–74. [[CrossRef](#)]
80. Roloff, A.; Gillner, S.; Kniesel, R.; Zhang, D. Interesting and new street tree species for European cities. *Jflr* **2018**, *3*, 1–7. [[CrossRef](#)]
81. Stratopoulos, L. “Klimabäume” für die Stadt. Über die Rolle Einer Angepassten Arten- und Sortenwahl für die Kühlleistung von Straßenbäumen. Ph.D. Thesis, Technische Universität München, Weihenstephan, Germany, 2020.
82. Stratopoulos, L.M.F.; Zhang, C.; Duthweiler, S.; Häberle, K.-H.; Rötzer, T.; Xu, C.; Pauleit, S. Tree species from two contrasting habitats for use in harsh urban environments respond differently to extreme drought. *Int. J. Biometeorol.* **2019**, *63*, 197–208. [[CrossRef](#)]
83. Smitley, D.R.; Peterson, N.C. Interactions of Water Stress, Honeylocust Spider Mites (Acari: Tetranychidae), Early Leaf Abscission, and Growth of *Gleditsia tncanthos*. *J. Econ. Entomol.* **1996**, *89*, 1577–1581. [[CrossRef](#)]

84. Klisz, M.; Puchałka, R.; Netsvetov, M.; Prokopuk, Y.; Vítková, M.; Sádlo, J.; Matisons, R.; Mionskowski, M.; Chakraborty, D.; Olszewski, P.; et al. Variability in climate-growth reaction of *Robinia pseudoacacia* in Eastern Europe indicates potential for acclimatisation to future climate. *For. Ecol. Manag.* **2021**, *492*, 119194. [[CrossRef](#)]
85. Moser-Reischl, A.; Rahman, M.A.; Pauleit, S.; Pretzsch, H.; Rötzer, T. Growth patterns and effects of urban micro-climate on two physiologically contrasting urban tree species. *Landsch. Urban Plan.* **2019**, *183*, 88–99. [[CrossRef](#)]
86. Netsvetov, M.; Prokopuk, Y.; Puchałka, R.; Koprowski, M.; Klisz, M.; Romenskyy, M. River Regulation Causes Rapid Changes in Relationships Between Floodplain Oak Growth and Environmental Variables. *Front. Plant Sci.* **2019**, *10*, 96. [[CrossRef](#)]
87. Thomsen, S.; Reisdorff, C.; Gröngroft, A.; Jensen, K.; Eschenbach, A. Responsiveness of mature oak trees (*Quercus robur* L.) to soil water dynamics and meteorological constraints in urban environments. *Urban Ecosyst.* [[CrossRef](#)]
88. Dervishi, V.; Poschenrieder, W.; Rötzer, T.; Moser-Reischl, A.; Pretzsch, H. Effects of Climate and Drought on Stem Diameter Growth of Urban Tree Species. *Forests* **2022**, *13*, 641. [[CrossRef](#)]